Sustain. Water Resour. Manag. (2015) 1:253–262
DOI 10.1007/s40899-015-0021-8

ORIGINAL ARTICLE

Hydrogeochemical and geomorphological investigation of travertine deposition in the Garab Spring region, NE Iran

Mohammad Reza Mansouri Daneshvar[1,2,3] · **Maliheh Pourali**[4]

Received: 28 August 2015 / Accepted: 31 August 2015 / Published online: 15 September 2015

Abstract In this research, the hydrogeochemical and geomorphological evidences of travertine deposition were investigated to detect the Garab Spring region as a unique travertine zone of northeastern Iran. Some of the hydrological and geochemical properties of the water and rocks were analyzed. According to the concentration of major components, the chemical property of the Garab Spring water was identified as Na–Cl and Ca–HCO_3–SO_4. Based on the geochemical results of XRF, the most important compositions of the rock samples were demonstrated as CaO, Fe_2O_3 and MgO with 59.24, 8.78 and 7.14 %, respectively. The petrography analysis indicated calcite mineralogy. Furthermore, the geomorphological shapes of the rocks were categorized into both robust travertine and fragile tufa.

Keywords Hydrogeochemical properties · Geomorphology · Travertine deposition · Garab Spring region

✉ Mohammad Reza Mansouri Daneshvar
mrm_daneshvar2012@yahoo.com

Maliheh Pourali
maliheh.pourali@stu.um.ac.ir

[1] Department of Environment and Urban Planning, Barzin–Mehr Land Evaluators Engineering Consultancy, Mashhad, Iran

[2] Department of Physical Geography and Climatology, University of Sistan and Baluchestan, Zahedan, Iran

[3] Department of Physical Geography and Geomorphology, Mashhad Branch, Islamic Azad University, Mashhad, Iran

[4] Department of Physical Geography, Ferdowsi University of Mashhad, Mashhad, Iran

Introduction

Travertine deposits as the chemical sedimentary rocks are mostly formed around seepages and springs and along streams with a complex internal architecture frequently changing both in lateral and vertical directions. The mentioned complexity originates from many factors such as spring position, underlying topography, chemical composition of travertine depositing waters, organic activity and surficial waters (Özkul et al. 2002). Travertine deposits are commonly Quaternary or Plio-Quaternary in age. They mostly crop out at the vicinities of Neotectonic structural features and are formed by the deposition of rising carbonate solutions through fissures (Akin 2010). Travertine forms in a wide variety of hydrogeological settings differ into numerous classes of geomorphological feature (Chafetz and Folk 1984; Pentecost and Viles 1994). Travertine deposition from thermal springs has been widely described in many parts of the world such as in Turkey (Altunel and Hancock 1993; Atabey 2002; Bayari et al. 2009), in Italy (Minissale et al. 2002; Anzalone et al. 2007; Brogi and Capezzuoli 2009; Petitta et al. 2011; Brogi et al. 2010), in Spain (Martín-Algarra et al. 2003) and in USA (Chafetz and Guidry 2003; Hershey et al. 2010). In the present study, the main aim is to detect the hydrological, geochemical and geomorphological properties of the Garab Spring region as a unique travertine zone of northeastern Iran.

Methodology

Study area

Based on the satellite images, the Garab Spring region is located geographically in the southeastern parts of

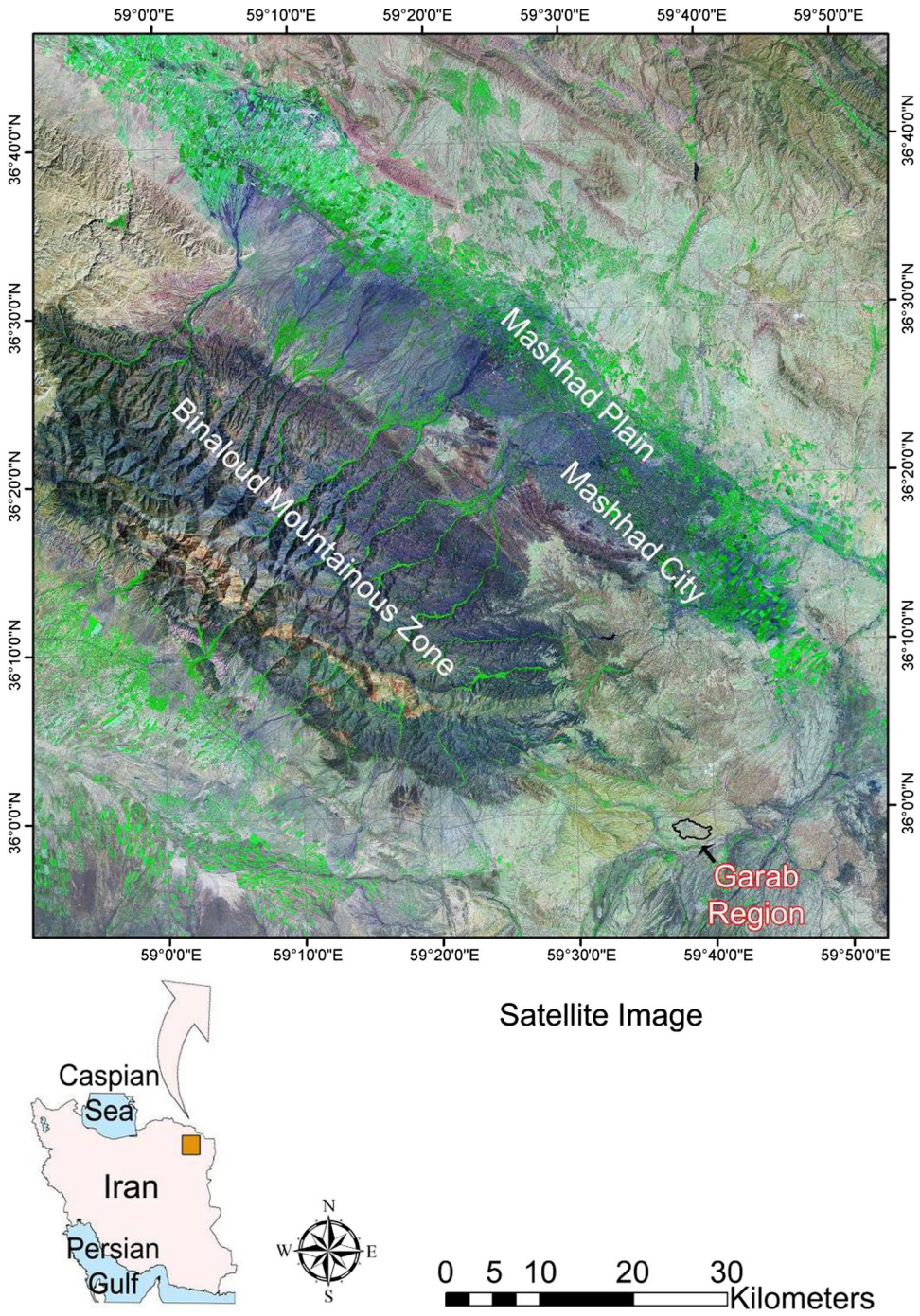

Fig. 1 Geographical position of the Garab Spring region on the satellite image

Binaloud mountainous zone, NE Iran (Fig. 1). This region has been emerged geologically among the Neogene conglomerates and Quaternary sediments, where it is affected by two extensional fault systems (Fig. 2). The Binaloud zone contains Paleo-Tethys remnants, including the Diorite, Meta-Flysch, Meta-Ophiolite and Granodiorite (Karimpour et al. 2010). The Garab region, with total surface area of about 5.8 km^2, lies between latitude 35.96°–36.00°N and longitude 59.60°–59.68°E. Topographically, the study area is made of a micro relief and mounded geo-form with mean elevation value of 1300 m a.s.l. along the geomorphological boundaries of Binaloud mountain and Mashhad plain (Fig. 3). There is a massive volcano-shaped cone, named main Garab Spring. Its exterior face and interior structure are shown in Fig. 4a and b. Furthermore, some of the bubble mineral springs of the region with mean flow of ~2 l/s are shown in Fig. 4c and d.

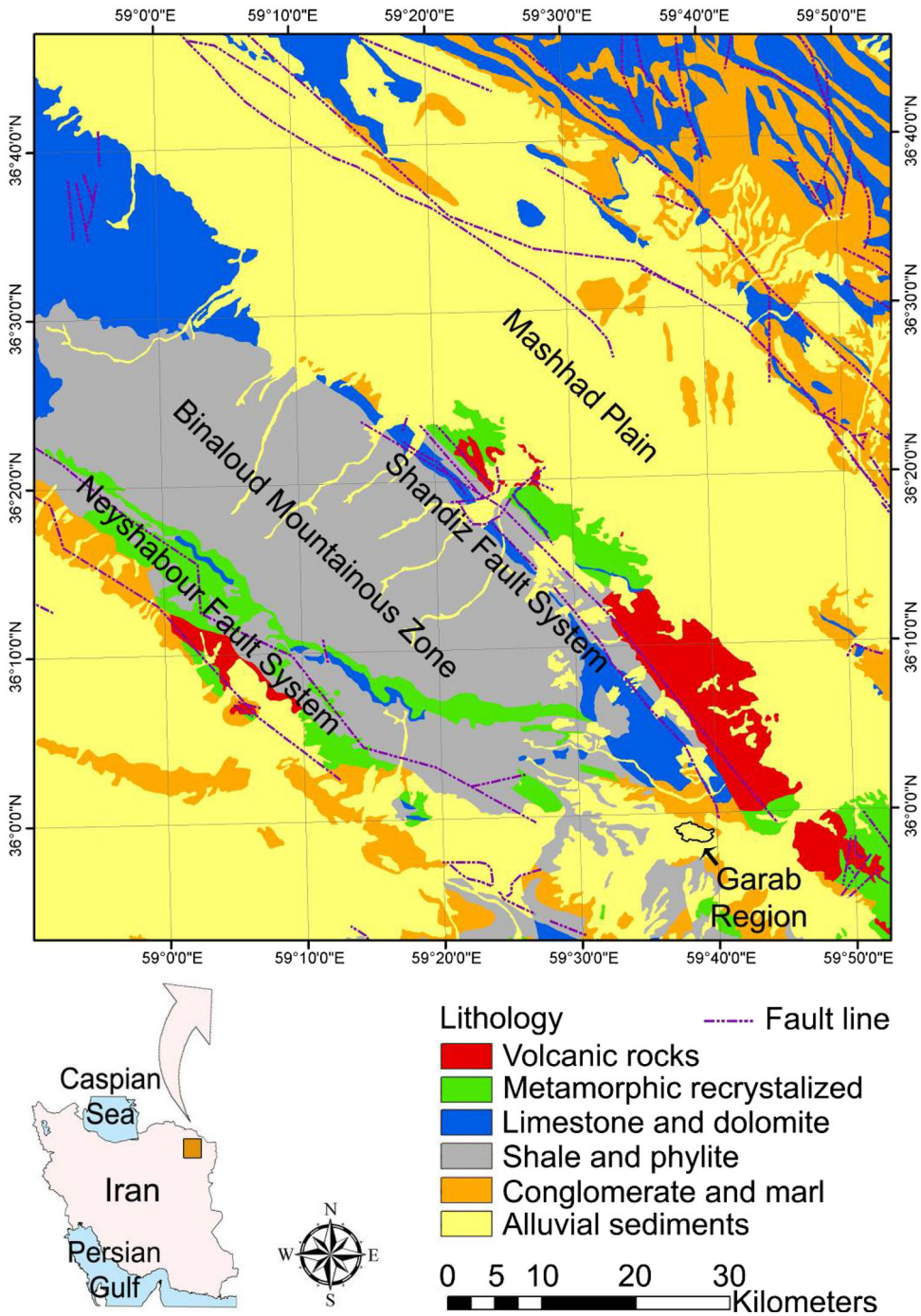

Fig. 2 Geological map and structural survey of the study area

Data preparation

In the hydrogeochemical analysis of the Garab Spring, the rock and water samples were gathered during a fieldwork on October 2011. The physical and chemical dataset of water samples were obtained by in situ measurements and laboratory analysis. Firstly, about 14 hydrological and 8 geochemical components were obtained. Field measurements of pH, EC and free CO_2 were carried out at the sampling site. The concentrations of other components were determined at the laboratory. The data scales were detected by logical procedures in Iran such as presented by Keshavarzi et al. (2011) and Pazand et al. (2012). Calcium (Ca^{2+}) and magnesium (Mg^{2+}) components were determined using ethylene diamine tetraacetic acid (EDTA). Chloride (Cl^{-}) component was determined by standard $AgNO_3$ titration method. Carbonate CO_3^{2-} and bicarbonate (HCO^{-3}) components were determined by titration of

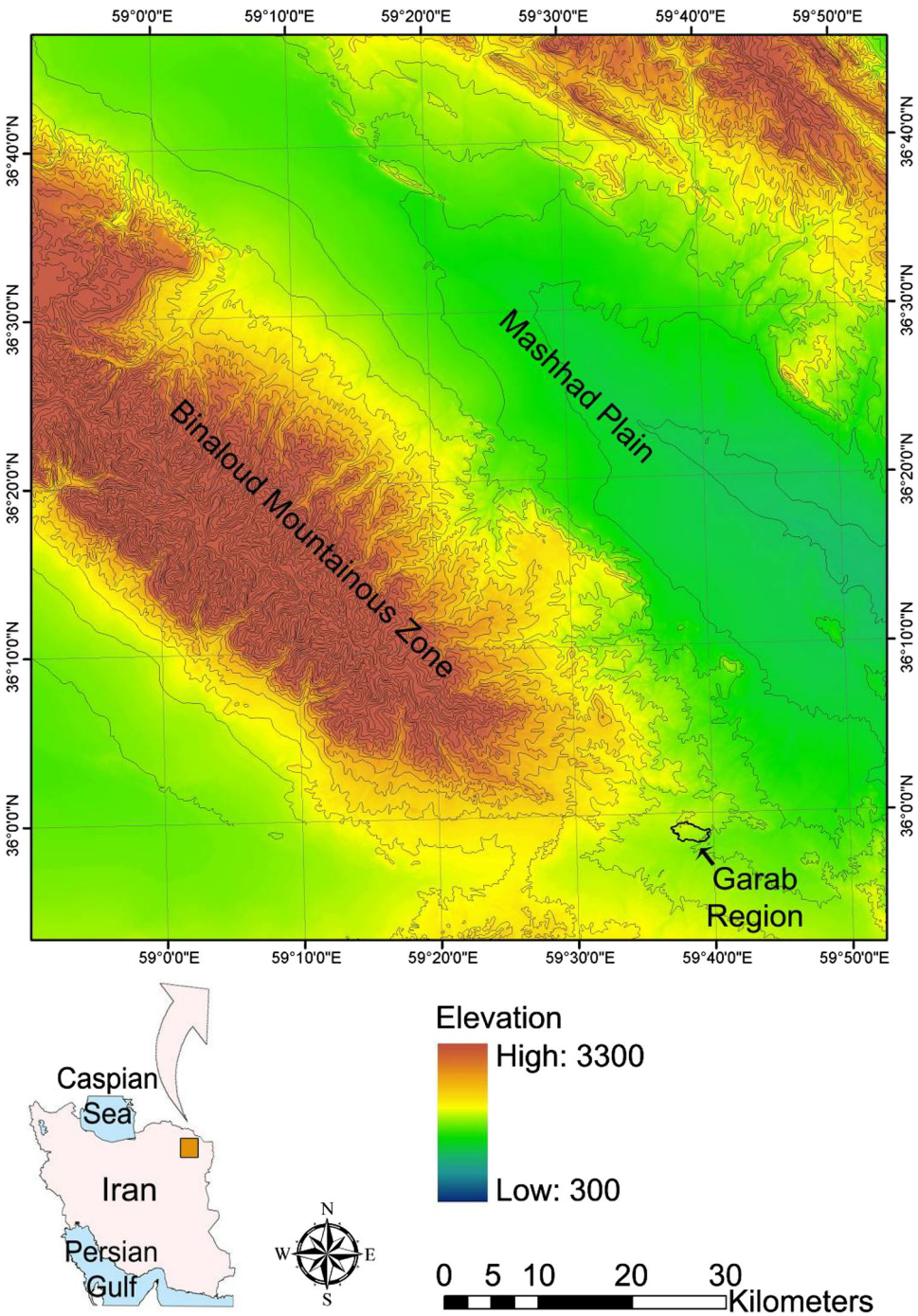

Fig. 3 Topographical characteristic of the study area

HCl. Sodium (Na^+) and potassium (K^+) components were measured by flame photometry and sulfate SO_4^{2-} by spectrophotometric turbidimetry. In the geochemical study, some thin sections from some rock samples were prepared. Aforementioned thin sections were analyzed under a polarized microscope. After the surficial assessment of the samples, those were analyzed using petrochemical technique of X-ray fluorescence (XRF). The geomorphological analysis was done based on the physiographic forms and patches of deposits.

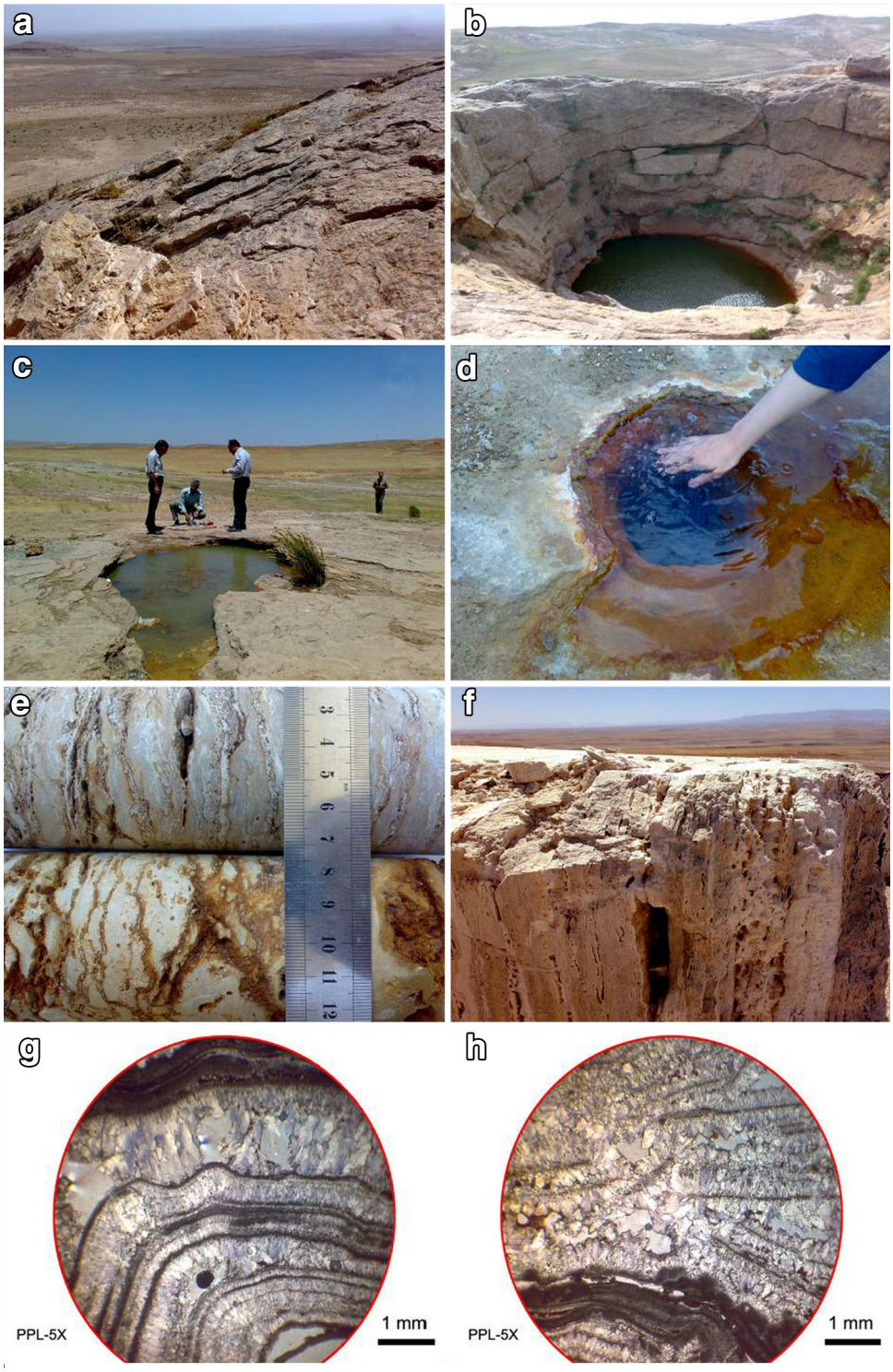

Fig. 4 **a** Exterior face of the massive shield of the Garab Spring, **b** the interior structure of the Garab Spring, **c** and **d** some of the bubble springs in the region, **e** and **f** the sampling rocks**, g** and **h** some of the thin sections from samples

Result and discussion

Hydrogeological analysis

In the present study, about 14 hydrological components were extracted from water samples as shown in Table 1. According to this table, the hydrogeochemical components of Na^+, Cl^-, HCO_3^- and SO_4^{2-} represented the dominant cation and anion with values of 2065, 2528, 1860 and 994 mg/l, respectively (total greater than 86 %). Total ion concentrations of Ca^{2+} and Mg^{2+} were about 510 mg/l, which could be the result of calcium carbonate and

dolomite (less than 12 %). According to the concentration of major cations and anions in Piper trilateral diagram (Piper 1944), the chemical property of the Garab aquifer was identified as Na–Cl and Ca–HCO_3–SO_4 (Fig. 5). All of the cations and anions display the following decreasing order: $Na^+ > Ca^{2+} > Mg^{2+} > K^+$ and $Cl^- > HCO_3^- > SO_4^{2-} > CO_3^{2-}$. The high concentrations of HCO_3^- and SO_4^{2-} as predominant anions in the water were attributed mainly to calcium carbonate rocks ($CaCO_3$) and gypsum lithology ($CaSO_4 \cdot 2H_2O$), but the concentration of Na^+ and Cl^- can be related to the saline soils (Na–Cl) or evaporitic strata in paths of upwelling water. According to the results, the mean values of silica (SiO_2) and CO_2 were recorded as 11 and 316 mg/l. Therefore, the values of pH and EC were recorded as 6.7 and 11000 µs/cm. Aforementioned recorded and estimated values were compared. Previously, Lastennet and Mudry (1997) have indicated that the concentrations of silica (SiO_2) and magnesium (Mg^{2+}) are tracers of the water from the deeper saturated ground. In the Pamukkale hydrothermal field in Turkey Dilsiz (2006) has revealed that the deep thermal waters with type of Ca–HCO_3–SO_4 have the richness of CO_2 (>150 mg/l). Recently, Liu et al. (2010) have exposed that the higher temperatures in deep ground waters can release more CO_2. Accordingly, the Garab region can be related to carbonate process by saturated calcite in deep ground (Mansouri Daneshvar 2015). In this regard, total dissolved solid (TDS) value and total hardness (TH) of spring water were estimated as 6930 and 1444 mg/l, respectively. According

Table 1 Hydrological components of water samples

No.	Unit	Component	Value
1	mg/l	Ca^{2+}	410
2	mg/l	Mg^{2+}	102
3	mg/l	Na^+	2065
4	mg/l	Ka^+	125
5	mg/l	Cl^-	2528
6	mg/l	CO_3^{2-}	0.38
7	mg/l	HCO_3^-	1860
8	mg/l	SO_4^{2-}	994
9	pH	pH	6.7
10	µs/cm	EC	11,000
11	mg/l	CO_2	316
12	mg/l	SiO_2	11
13	mg/l	TDS	6930
14	mg/l	TH	1444

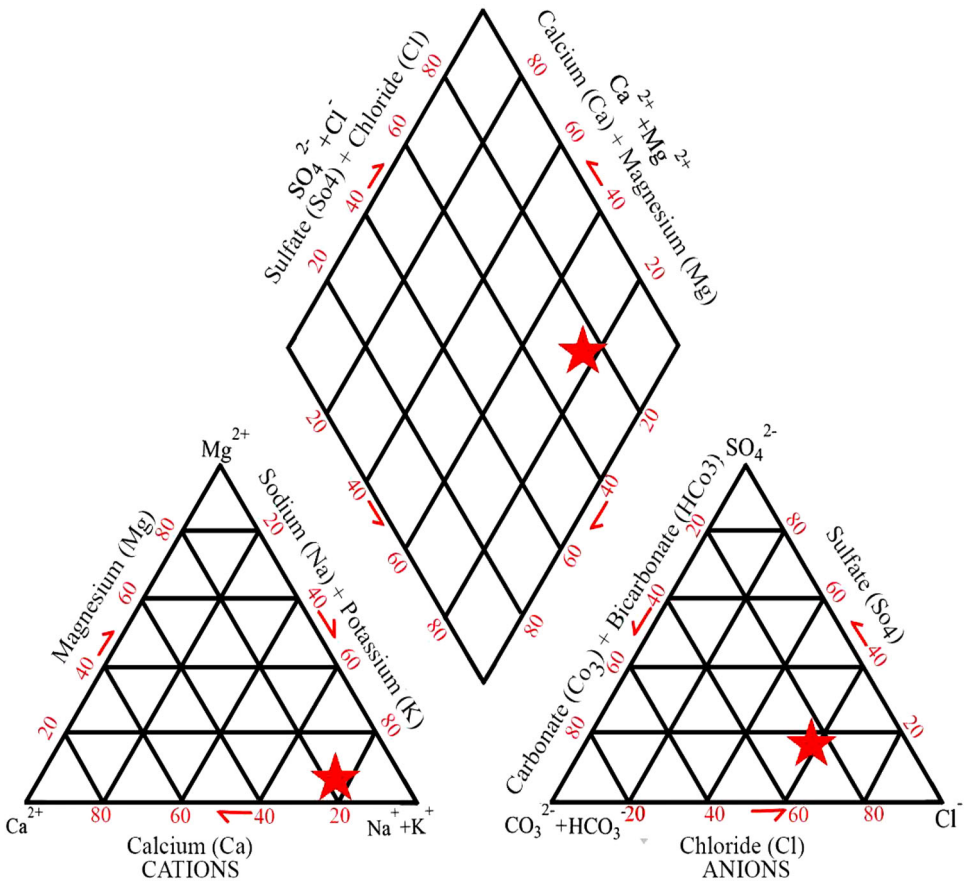

Fig. 5 Piper diagram of hydrogeochemical properties of Garab Spring

Table 2 Geochemical components of samples by XRF

No.	Component	Value (%)
1	SiO_2	2.18
2	TiO_2	1.02
3	Al_2O_3	0.15
4	Fe_2O_3	8.78
5	MgO	7.17
6	CaO	59.24
7	Na_2O	5.98
8	K_2O	5.23
9	Loss on ignition (LOI)	10.23
10	Total	99.98

to Özler (2000) the high TDS values can be related to geothermal waters. Furthermore, the high TDS content can be related to dissolution of carbonates from the calcareous rocks and leakage of the deep ground (Flores-Márquez et al. 2006).

Geochemical analysis

For detailed geochemical analysis, some thin sections were prepared from selected samples (Fig. 4e, f). These samples were used to illustrate the petrographical properties of the deposits in the region. Primary petrography indicated calcite mineralogy (Fig. 4g, h). Their veins have been filled by siderite and hematite injections attributed to highly porous texture. The calcite values from the thin sections averaged 60 % after the visual estimation. Based on the chemical results of XRF about 8 geochemical components were extracted from spring rock samples as shown in Table 2. According to the table, most compositions of the sample were demonstrated as CaO, Fe_2O_3 and MgO with 59.24, 8.78 and 7.14 %, respectively. In this regard, the main calcite mineralogy of carbonate rocks was detected based on the plot of CaO–MgO–SiO_2, MgO–Al_2O_3–SiO_2, and CaO–MgO–other compositions ternary diagrams (Fig. 6). Ternary diagrams are frequently used in geosciences to visualize compositional data characterized by three or more components, which are amalgamated to three components (Von Eynatten et al. 2002).

Geomorphological analysis

The contribution of tectonic activity and extensional fault systems are important considerations in the regional studies of travertine (Chafetz and Folk 1984; Hancock et al. 1999; Newell et al. 2005; Crossey et al. 2006). According to the hydrological and geochemical analysis, the Garab region is a travertine zone which has been limited by tectonics of

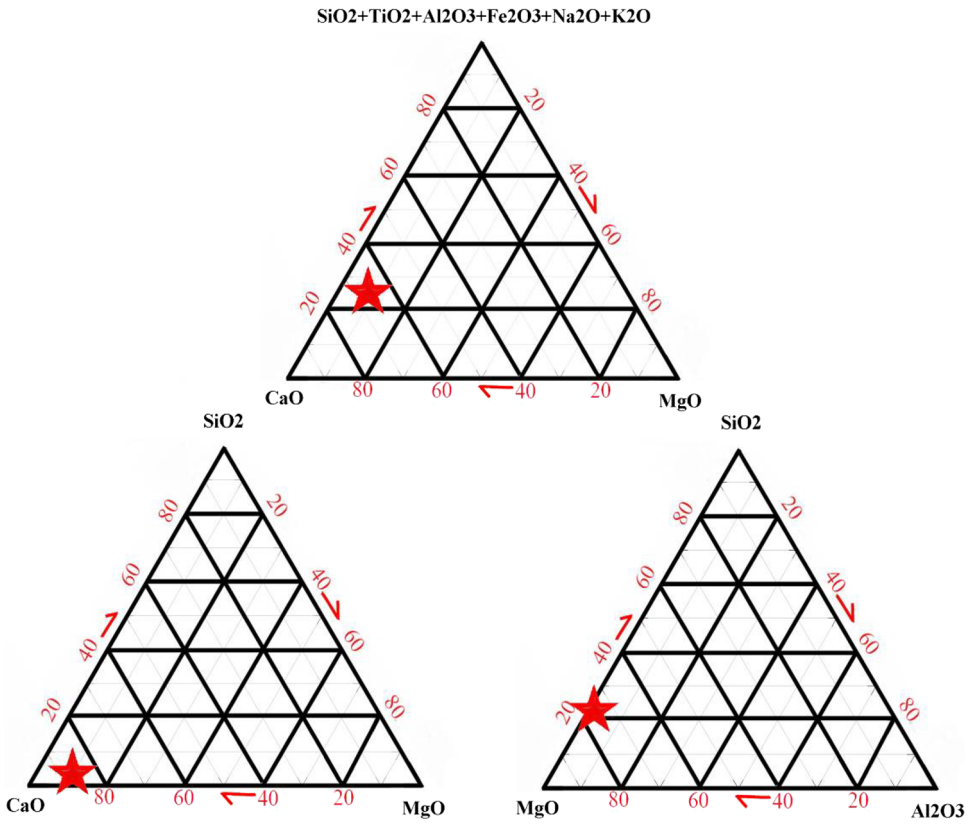

Fig. 6 Plot of main ternary diagrams of CaO–MgO–SiO_2, MgO–Al_2O_3–SiO_2, and CaO–MgO–other compositions for detecting the calcite mineralogy

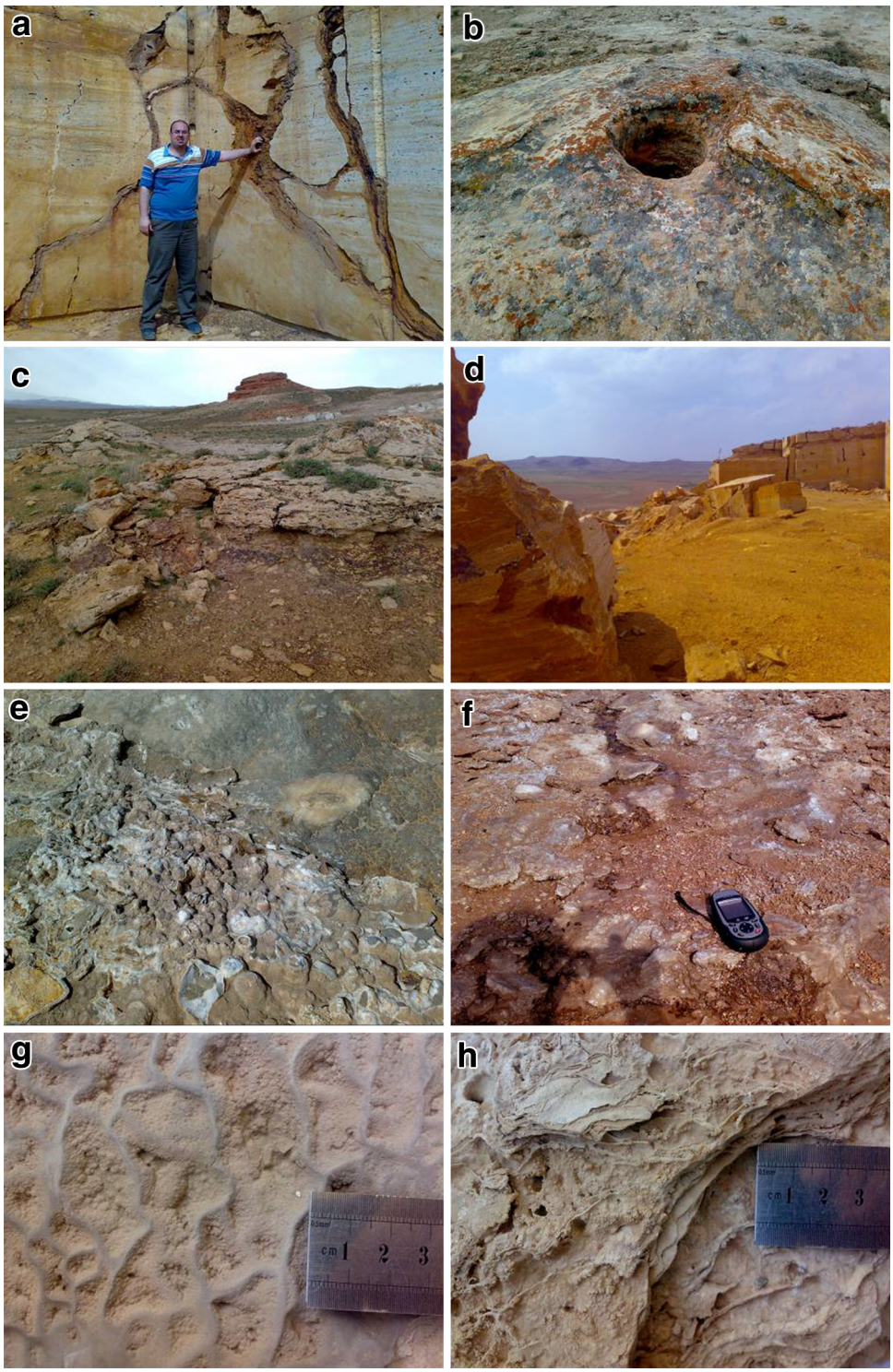

Fig. 7 **a** The profile of a massive robust travertine with vertical and horizontal veins, **b** a travertine cone, **c** and **d** travertine shields in the study area **e** and **f** in situ genesis of fragile tufa, **g** and **h** some of rust-colored deposits with imprints of leaves and natural material

two extensional faults of Neyshabour and Shandiz fault systems. In this regard, the Garab region can be categorized a travitonic zone. The term of travitonic is propounded to the relationship between travertine depositions and faulting (Hancock et al. 1999), suggesting that the age of travertine can be indicative of the age of faulting (Brogi et al. 2010). Therefore, a number of extensive chemical and physical conditions have produced a wide variety of friable meteogene tufa and massive thermogene travertine. According to the literature, regular bedding and fine lamination, low porosity, low permeability and inorganic crystalline fabrics are characterized as travertine rock, which can be related to thermal process (Shi et al. 2014). In contrast, the highly porous bodies, poor bedding lenticular

profiles and abundant remains of organic matters are characterized as the tufa deposits (Capezzuoli et al. 2013). In the study area, the geomorphological shapes of carbonate deposition were categorized into the both robust travertine (Fig. 7a–d) and fragile tufa (Fig. 7e, f). Outlying tufa deposits in the study area were frequently more porous, usually brown or rust colored and sometimes with imprints of leaves and natural material (Fig. 7g, h). The coexistence of tufa and travertine can result from shallow and deeply circulated waters in the fault damage zone (Brogi and Capezzuoli, 2009). Along the wall cut profiles of the massive travertine rocks, there are several vertical and horizontal veins that intersect each other repeatedly. Özkul et al. (2013) have examined the same geomorphology in Denizli basin.

Conclusion

The present study revealed the hydrogeochemical properties of the travertine rocks in the Garab Spring region, NE Iran. The hydrogeochemical components of Na^+, Cl^-, HCO_3^- and SO_4^{2-} presented dominant cation and anion with values of 2065, 2528, 1860 and 994 mg/l, respectively (total greater than 86 %). The chemical type of the Garab Spring water was identified as Na–Cl and Ca–HCO_3–SO_4. The mean value of silica (SiO_2) and CO_2 were recorded as 11 and 316 mg/l. Therefore, total dissolved solid (TDS) value and total hardness (TH) of spring water were estimated as 6930 and 1444 mg/l, respectively. In the study area, the values of EC (11,000 μs/cm), TDS (∼7000 mg/l) and CO_2 (∼320 mg/l) together with water type were attributed to travertine water origin. The evidence of carbonate rock including calcite mineralogy was detected based on the plot of main ternary diagrams. The calcite precipitations in the region are shown as both fragile tufa and robust travertine rocks. These types of carbonate rocks resulted from shallow and deeply circulated waters along the extensional fault systems of Binaloud zone. In this regard, the Garab region can be categorized a travitonic zone.

Acknowledgments

The author thanks three anonymous reviewers for technical suggestions on data interpretations.

References

Akin M (2010) A quantitative weathering classification system for yellow travertines. Environ Earth Sci 61:47–61

Altunel E, Hancock PL (1993) Morphology and structural setting of Quaternary travertines at Pamukkale, Turkey. Geol J 28(3–4):335–346

Anzalone E, Ferreri V, Sprovieri M, D'Argenio B (2007) Travertines as hydrologic archives: the case of the Pontecagnano deposits (southern Italy). Adv Water Resour 30(10):2159–2175

Atabey E (2002) The formation of fissure ridge type laminated travertine–tufa deposits microscopical characteristics and diagenesis, Kirşehir, central Anatolia. Bull Miner Res Explor Inst Turk 123–124:59–70

Bayari CS, Pekkan E, Ozyurt NN (2009) Obruks, as giant collapse dolines caused by hypogenic karstification in central Anatolia, Turkey: analysis of likely formation processes. Hydrogeol J 17(2):327–345

Brogi A, Capezzuoli E (2009) Travertine deposition and faulting: the fault–related travertine fissure–ridge at Terme S. Giovanni, Rapolano Terme (Italy). Int J Earth Sci 98(4):931–947

Brogi A, Capezzuoli E, Aqué R, Branca M, Voltaggio M (2010) Studying travertines for neotectonics investigations: middle-Late Pleistocene syn–tectonic travertine deposition at Serre di Rapolano (Northern Apennines, Italy). Int J Earth Sci 99(6):1383–1398

Capezzuoli E, Gandin A, Pedley M (2013) Decoding tufa and travertine (fresh water carbonates) in the sedimentary record: the state of the art. Sedimentology 61(1):1–21

Chafetz HS, Folk RL (1984) Travertines; depositional morphology and the bacterially constructed constituents. J Sediment Res 54(1):289–316

Chafetz HS, Guidry SA (2003) Deposition and diagenesis of Mammoth Hot springs travertine, Yellowstone National Park, Wyoming, USA. Can J Earth Sci 40(11):1515–1529

Crossey LJ, Fischer TP, Patchett PJ, Karlstrom KE, Hilton DR, Newell DL, Huntoon P, Reynolds AC, de Leeuw GAM (2006) Dissected hydrologic system at the Grand Canyon; interaction between deeply derived fluids and plateau aquifer waters in modern springs and travertine. Geology 34(1):25–28

Dilsiz C (2006) Conceptual hydrodynamic model of the Pamukkale hydrothermal field, southwestern Turkey, based on hydrochemical and isotopic data. Hydrogeol J 14(4):562–572

Flores–Márquez EL, Jiménez-Suárez G, Martínez-Serrano RG, Chávez RE, Silva-Pére D (2006) Study of geothermal water intrusion due to groundwater exploitation in the Puebla Valley aquifer system, Mexico. Hydrogeol J 14(7):1216–1230

Hancock PL, Chalmers RML, Altunel E, Çakir Z (1999) Travitonics: using travertines in active fault studies. J Struct Geol 21(8–9):903–916

Herhsey RL, Mizell SA, Earman S (2010) Chemical and physical characteristics of springs discharging from regional flow systems of the carbonate–rock province of the Great Basin, western United States. Hydrogeol J 18(4):1007–1026

Karimpour MH, Stern CR, Farmer GL (2010) Zircon U-Pb geochronology, Sr–Nd isotope analyses, and petrogenetic study of the Dehnow diorite and Kuhsangi granodiorite (Paleo–Tethys), NE Iran. J Asian Earth Sci 37:384–393

Keshavarzi B, Moore F, Mosaferi M, Rahmani F (2011) The source of natural arsenic contamination in groundwater, west of Iran. Water Quality Exposure Health 3:135–147

Lastennet R, Mudry J (1997) Role of karstification and rainfall in the behavior of a heterogeneous karst system. Environ Geol 32(2):114–123

Liu Z, Sun H, Baoying L, Xiangling L, Wenbing Y, Cheng Z (2010) Wet–dry seasonal variations of hydrochemistry and carbonate precipitation rates in a travertine–depositing canal at Baishuitai, Yunnan, SW China: implications for the formation of biannual laminae in travertine and for climatic reconstruction. Chem Geol 273(3–4):258–266

Mansouri Daneshvar MR (2015) Climatic impacts on hydrogeochemical characteristics of mineralized springs: a case study of the Garab travertine zone in the northeast of Iran. Arabian J Geosci 8(7):4895–4906

Martín-Algarra A, Martín-Martín M, Andreo B, Julià R, González-Gómez C (2003) Sedimentary patterns in perched spring travertines near Granada (Spain) as indicators of the palaeohydrological and palaeoclimatological evolution of a karst massif. Sed Geol 161(3–4):217–228

Minissale A, Kerrick DM, Magro G, Murrell MT, Paladini M, Rihs S, Sturchio NC, Tassi F, Vaselli O (2002) Geochemistry of Quaternary travertines in the region north of Rome (Italy): structural, hydrologic and paleoclimatic implications. Earth Planet Sci Lett 203(2):709–728

Newell DL, Crossey LJ, Karlstrom KE, Fischer TP, Hilton DR (2005) Continental–scale links between the mantle and groundwater systems of the Western United States; evidence from travertine springs and regional He isotope data. GSA Today 15(12):4–10

Özkul M, Varol B, Alçiçek MC (2002) Depositional environments and petrography of denizli travertines. Mineral Res Explor Bull 125:13–29

Özkul M, Kele S, Gökgöz A, Shen CC, Jones B, Baykara MO, Fórizs I, Németh T, Chang YW, Alçiçek MC (2013) Comparison of the Quaternary travertine sites in the Denizli extensional basin based on their depositional and geochemical data. Sed Geol 294:179–204

Özler HM (2000) Water balance and water quality in the Çürüksu basin, western Turkey. Hydrogeol J 7(4):405–418

Pazand K, Hezarkhani A, Ghanbari Y, Aghavali N (2012) Groundwater geochemistry in the Meshkinshahr basin of Ardabil province in Iran. Environ Earth Sci 65:871–879

Pentecost A, Viles H (1994) A review and reassessment of travertine classification. Géog Phys Quatern 48(3):305–314

Petitta M, Primavera P, Tuccimei P, Aravena R (2011) Interaction between deep and shallow groundwater systems in areas affected by Quaternary tectonics (Central Italy): a geochemical and isotope approach. Environ Earth Sci 63(1):11–30

Piper AM (1944) A graphic procedure in the geochemical interpretation of water analysis. Trans Am Geophys Union 25(6):914–923

Shi Z, Shi Z, Yin C, Liang J (2014) Travertine deposits, deep thermal metamorphism and tectonic activity in the Longmenshan tectonic region, southwestern China. Tectonophysics 633:156–163

Von Eynatten H, Pawlowsky-Glahn V, Egozcue JJ (2002) Understanding perturbation on the simplex: a simple method to better visualize and interpret compositional data in ternary diagrams. Math Geol 34(3):249–257